On the distribution of zeros of chaotic wavefunctions

1997 J. Phys. A: Math. Gen. 30 6313

(http://iopscience.iop.org/0305-4470/30/18/014)

J. Phys. A: Math. Gen. **30** (1997) 6313–6326. Printed in the UK PII: S0305-4470(97)81325-X

On the distribution of zeros of chaotic wavefunctions

Pragya Shukla

Condensed Matter Theory Unit, Jawaharlal Nehru Centre for Advanced Scientific Research, Indian Institute of Science, Bangalore-560012, India

Received 27 January 1997

Abstract. Wavefunctions in a phase-space representation can be expressed as entire functions of their zeros if the phase space is compact. These zeros seem to hide a lot of relevant and explicit information about the underlying classical dynamics. Besides, an understanding of their statistical properties may prove to be useful in the analytical calculations of the wavefunctions in quantum-chaotic systems. This motivates us to pursue the present study which by a numerical statistical analysis shows that both long-range correlations as well as short-range correlations exist between zeros; while the latter turn out to be universal and parametric independent, the former seem to be system dependent and are significantly affected by various parameters, i.e. symmetry, localization, etc. Furthermore, for the delocalized quantum dynamics, the distribution of these zeros seem to mimic that of the zeros of the random functions as well as random polynomials.

1. Introduction

In this paper, our aim is to study the statistical distribution of zeros of 'quantum chaotic' wavefunctions, expressed in a phase-space representation. The wavefunctions of quantum-chaotic systems have so far remained a relatively less explored (as compared with spectra) area notwithstanding their importance in quantum mechanical as well as semi-classical analysis. Their few known properties are the microcanonical nature of wavefunctions if the underlying classical dynamics is chaotic [1], the scarring behaviour [2, 3] and dynamical localization [4] or a few statistical (numerical) studies of the components of these wavefunctions [5, 6]. The relevant information hidden in the semiclassical wavefunction about the underlying quantum-classical correspondence is not yet fully extracted. This motivates us to pursue the present problem. As intuition suggests, this can be studied best by analysing various properties of the wavefunctions in the phase space where quantum dynamics in the limit $\overline{h} \to 0$ can be compared with the underlying classical dynamics. One such analysis involves the study of the distribution of zeros (or nodal patterns) of wavefunctions (in a phase-space representation).

The interest in the phase-space study of the nodal patterns arises following a study by Leboeuf and Voros [7, 8] where they showed that the coherent-state representation of a wavefunction (i.e. Bargmann or Husimi function) has a finite number N of zeros in phase space (N being the dimension of Hilbert space) and the state of the system can be completely expressed in terms of these zeros. Furthermore, their numerical studies on quantum maps (e.g. Baker and kicked rotor) have also revealed that the zeros, in the semiclassical regime $\overline{h} \to 0$, condense on lines for classically integrable systems whereas for strongly chaotic quantum maps they appear to diffuse fairly uniformly over the phase space; this behaviour

0305-4470/97/186313+14$19.50

can be explained semiclassically [7, 8]. The only exception to this behaviour, so far, has been seen for one eigenfunction in the $N = 2^k$ case of the Baker map (strongly chaotic) where zeros have a dominantly linear distribution. In general, the distribution of zeros seems to mimic the underlying classical dynamics in semiclassical limit (for example for those chaotic cases of the kicked rotor, where quantum dynamics is localized in momentum space, zeros were observed to be localized). This makes it relevant to seek further information about their behaviour.

In principle, we have an analytical formulation available to write the eigenfunction directly in a nodal pattern representation (a polynomial for spherical phase space and a complicated function for torus and cylindrical phase space) [7]. But this formulation does not help us very much as it depends on the knowledge of the position of each zero in phase space which is analytically difficult to evaluate. Still it can be used to determine the statistical behaviour of the eigenfunctions if the statistical properties of zeros are known.

The random nature of a chaotic wavefunction and its polynomial form in the Bargmann representation (in a spherical phase space only) has motivated people to seek analogy between the distribution of its zeros and roots of random polynomials (RP) [9]; recently we analytically explored [10] the statistical properties of the latter case. Our results showed an excellent agreement with the corresponding ones for the kicked top and kicked rotor. It was a little surprising in the latter case where dynamics was confined to a torus and an arbitrary wavefunction was a complicated function instead of a polynomial; one should expect the zeros of random functions (superposition of functions with random weight, later referred to as RF) to be a better model. This seemed to hint that the zeros, while distributing themselves in the semiclassical limit, do not distinguish between spherical and torus phase space [10]. In other words, the zeros of RF and RP seem to have the same distribution properties. As we show in this paper, this is indeed the case. We also extend the above study to understand the effect of various parameters (i.e. symmetry breaking, localization, etc) on the distribution of zeros. We expect this due to our prior knowledge of the significant influence of these parameters on quantum dynamics [4, 11, 12].

We choose the kicked rotor system for this purpose as it has been an active model of research, containing a variety of features such as localization, resonance, dependence of the spectra on number theoretical properties, etc and has been used as a model for a very wide range of physical systems [4]. Besides, the kicked rotor can also display discrete symmetries such as parity and time reversal [5, 11, 12]. This will enable us to study the way these symmetries reveal themselves in the distribution of zeros.

This paper is organized as follows. Section 2 contains a brief review of quantum properties of kicked rotor. Section 3 briefly describes the various phase-space representations and their advantages over each other. Section 4 deals with the numerical analysis of the distribution of zeros for kicked rotor for various parametric conditions, followed by a conclusion in section 5.

2. The kicked rotor: Classical and quantum dynamics

The kicked rotor can be described as a pendulum subjected to periodic kicks (with period T) with the following Hamiltonian

$$H = \frac{(p+\gamma)^2}{2} + \frac{K}{4\pi^2}\cos(2\pi\theta + \theta_0)\sum_{n=-\infty}^{\infty}\delta(t - nT) \tag{1}$$

where K is the stochasticity parameter. Parameters γ and θ_0 are introduced in the Hamiltonian in order to mimic the effects of the time-reversal (T) and the parity (P)

symmetry breaking in the quantum Hamiltonian while acting in a finite Hilbert space.

Floquet's theorem enables us to describe the related quantum dynamics by a discrete time-evolution operator $U = GBG$ where $B = \exp(-\mathrm{i}K\cos(2\pi\theta + \theta_0)/4\pi^2\overline{h})$ and $G = \exp(-\mathrm{i}(p+\gamma)^2/4\overline{h})$. Here θ and p are position and momentum operators respectively, with p having discrete eigenvalues $p|l\rangle = l\overline{h}|l\rangle$ due to the periodicity of $\theta(\theta = \theta + 2\pi)$. The nature of the quantum dynamics and therefore the statistical properties of the associated quantum operators depend on $\overline{h}$ and K. The choice of a rational value for $\overline{h}T/2\pi$ results in a periodicity also for the momentum space ($p = p + 2\pi M$ or $l = l + N$) and, therefore, in discrete eigenvalues for $\theta(\theta|n\rangle = \frac{2\pi n}{M}|n\rangle)$. The quantum dynamics can then be confined to a two-dimensional torus (with finite Hilbert space of dimension N) and U can be reduced to a finite N-dimensional matrix of the form [7, 4]

$$U_{mn} = \frac{1}{N^2}\sum_j \exp\left[-\mathrm{i}\frac{K}{4\pi^2\overline{h}}\cos\left(\frac{2\pi j}{N} + \theta_0\right)\right]\sum_{l,l'=-N_1}^{N_1}\exp[-\mathrm{i}(\pi^2\overline{h}(l^2 + l'^2) - \pi\gamma(l + l'))]$$
$$\exp\left[-\mathrm{i}\left(\frac{l(m-j) + l'(j-n)}{N}\right)\right] \tag{2}$$

where $N_1 = (N-1)/2$ (with N odd) and $m, n = -N_1, -N_1 + 1, \ldots, N_1$.

In contrast to the classical dynamics, the quantum dynamics can be significantly affected by the relative values of three parameters, namely, K, $\overline{h}$ and N. It has already been pointed out [4] that, for $K^2 > N\overline{h}^2 (= 2\pi M/T)$, the eigenstates are fully extended in momentum space (later referred to as the delocalized case); it is also called the strong chaos limit as here the kick is strong enough to make the classical motion ergodic in all of the phase space [12]. We also know that the spectrum, as well as the distribution of eigenvector components in this case, with parameters γ and θ_0 chosen to preserve either exact or partially violated symmetry, can be modelled by the random matrix theories (RMT) [5, 6, 11, 12]. Under this limit, the quantum dynamics has a time-reversal symmetry T for $\gamma = 0$ and a parity symmetry P for $\theta_0 = 0$. Although the T-symmetry may be violated for $\gamma \neq 0$, still a more generalized antiunitary symmetry $S = TP = PT$ can be preserved in the system if $\theta_0 = 0$ [5, 11]. By a slow variation of these parameters, one can realize the various intermediate stages of the statistical properties of quantum operators, for example, the Poisson $\rightarrow$ COE transition of the spectrum for K-variation, COE $\rightarrow$ CUE for γ-variation with θ_0 fixed at a non-zero value etc. In the opposite limit of weak chaos, namely, $K^2 \ll N\overline{h}^2$ (corresponding to a diffusively covered phase space with a non-uniform distribution of periodic orbits), the eigenstates localize in the momentum space and one obtains a Poisson distribution for the spectrum (later referred to as the localized case). Moreover, here the symmetry breaking may not be realized in the quantum dynamics just by making θ_0 or γ sufficiently non-zero.

3. The phase-space representations of wavefunctions

The phase space representation of the eigenfunctions of quantum mechanical operators can give excellent information about the semiclassical description of a quantum state. A semiclassical wavefunction can be constructed, first by writing the quantum state as a function of the parameter $\overline{h}$, and then by exploiting the fact that this function should approach the corresponding classical function in the limit $\overline{h} \rightarrow 0$ [13]. This is easily observed in the phase-space representation of quantum state, where the quantum dynamics (the Heisenberg equation), analysed in terms of density operator $\rho = |\psi\rangle\langle\psi|$, explicitly appears as a deformation of classical dynamics (the Liouville equation). This enables one to compare the quantum function with the corresponding classical function, order by order

in $\overline{h}$. The inversion $W \to \psi$ then gives, in principle, the quantum state for various orders in $\overline{h}$. The two most widely used phase-space techniques are the Wigner representation W_w defined as

$$W_w(q, p, \overline{h}) = (2\pi\overline{h})^{-N} \int \psi\left(q - \frac{r}{2}\right) \psi\left(q + \frac{r}{2}\right) \mathrm{e}^{\mathrm{i}pr/\overline{h}}\, \mathrm{d}^N r \tag{3}$$

and the Husimi representation W_h given as

$$W_h(q, p, \overline{h}) = \frac{|\langle z|\psi\rangle|^2}{\langle z|z\rangle} \tag{4}$$

where $|z\rangle$ is a plane coherent state described by following standard formulae,

$$|z\rangle = \mathrm{e}^{\bar{z}a^+}|0\rangle \qquad a^+ = \frac{(\hat{q} - \mathrm{i}\hat{p})}{\sqrt{2\overline{h}}} \qquad z = \frac{q - \mathrm{i}p}{\sqrt{2}} \tag{5}$$

with q and p being the position and momentum eigenvalues of the operator $\hat{q}$ and $\hat{p}$ respectively and its overlap with position wavefunction given as follows

$$\langle q|z\rangle = (\pi\overline{h})^{-N/4} \exp[-(\hat{z}^2 + q^2) + \sqrt{2}\hat{z}q/\overline{h}]. \tag{6}$$

Both of these representations have a nice semiclassical behaviour, converging to the classical phase-space distribution in the limit $h \to 0$. But the determination of this convergent form of W_w and W_h can be done only after smoothing out the oscillations (stronger in the case of W_w) existing in both cases. In general, however (i.e. for chaotic cases) even this knowledge is not sufficient to reconstruct the wavefunction itself by inverting the map $W \to \psi$. The reason is that the quantum phase, which controls the fast oscillations, is obliterated in the limiting process and cannot be easily regenerated. Moreover, these representations also run into difficulties when applied to compact phase spaces. It is because the existence and uniqueness of the construction of the Wigner representation, which imposes itself by symmetry on a linear phase space, is no longer clear on a compact space [7]. One does not face these difficulties with the Husimi representation which only needs coherent states. But the usual plane coherent state, used in Husimi formulation, becomes non-analytic when restricted to a compact space [7]. Thus, for our purpose, we should choose a coherent state with analytical properties in compact space.

As discussed in [7], the analyticity of the quantum state can be preserved by expressing it in the 'Bargmann representation'. This representation diagonalizes the creation operator $\hat{z}$ and expresses a state as a function $\psi(z) = \langle z|\psi\rangle$ with $\hat{z}^+ = \overline{h}\frac{\mathrm{d}}{\mathrm{d}z}$ (similar to the Schrödinger representation $\psi(q)$ of the quantum state, obtained by diagonalizing the position operator $\hat{q}$ with $\hat{p} = -\mathrm{i}\overline{h}\frac{\mathrm{d}}{\mathrm{d}q}$). The function $\psi(z)$, describing the overlap of wavefunction ψ with the coherent state $|z\rangle$, belongs to a Hilbert space of entire (analytic) functions with the finite norm given as follows

$$\langle\psi(z)|\psi(z)\rangle = (2\pi\overline{h})^{-1} \int |\psi(z)|^2 \mathrm{e}^{-|z|^2/\overline{h}}\, \mathrm{d}q\, \mathrm{d}p. \tag{7}$$

Furthermore the Husimi function can be expressed in terms of $\psi(z)$ as $W_H = |\langle z|\psi\rangle|^2/\langle z|z\rangle$. Thus, one can consider $\psi(z)$ as a sort of phase-space representation for the wavevector $|\psi\rangle$. The advantage of working with $\psi(z)$ is that it preserves the information about the quantum phase explicitly.

It was shown in [7] that the antianalytic coherent states for compact space such as the torus (the case considered here) can be obtained by applying periodic boundary conditions on the antianalytic coherent states $|z\rangle$ on the plane. Thus, the imposition of the appropriate periodic boundary conditions on the kernel (4), depending on the nature of the compact

space, leads to a Hilbert space of entire functions $\psi(z)$. For our purpose, we only mention here the case of the torus, where application of the periodic boundary conditions in both the q as well as p directions and use of the condition $2\pi N\overline{h} = 1$ results in the following form for $\psi(z)$

$$\psi(z) = \sum_{n=0}^{N-1} \psi(q_n)\langle\langle z|q_n\rangle\rangle \tag{8}$$

where ψ_n's are the eigenfunctions of operator U in the coordinate representation and $\langle\langle z|q_n\rangle\rangle$ is the projection of the coordinate eigenfunction $|q_n\rangle$ in the z-space, under the periodic boundary conditions

$$\langle\langle z|q_n\rangle\rangle = (2N)^{1/4}\exp[-2\pi N(z^2+q_n^2)/2 - \sqrt{2}zq_n]\theta_3\left(\mathrm{i}\pi N\left[q_n - \mathrm{i}\frac{\theta_q}{2\pi N} - z\sqrt{2}\right]|\mathrm{i}N\right). \tag{9}$$

Here coefficients $\psi(q_n)$'s are complex under no-symmetry condition. But the presence of a T-symmetry makes them real as now if $\psi(z_p) = 0$ then $\psi(Tz_p) = 0$ too [10]. The existence of an additional symmetry such as parity imposes further restrictions on $\psi(q_n)$'s; $\psi(q_n) = 0$ if n is odd and $\psi(q_n) \neq 0$ if n is even. Further, by using the periodic boundary conditions leading to this compact space, it can be shown [7] that every function $\psi(z)$ has exactly N zeros in the fundamental domain (defined by $\delta q = 1$, $\delta p = 1$).

It is worth reminding ourselves here that, for a spherical phase space, $\langle\langle z|q_n\rangle\rangle$ takes the form of a polynomial [7] and therefore the choice of $\psi(q_n)$'s as a Gaussian random variables leaves $\psi(z)$ as a random polynomial. In [10], we analytically calculated the joint probability density of these zeros as well as the correlation function and compared the result with numerical results for kicked top (which has a spherical phase space); we found a good agreement. But as is obvious from equation (9), for a torus phase space, $\psi(z)$ is not a polynomial. A choice of $\psi(q_n)$'s as random variables gives rise to a random function (later referred to as RFC for complex and random coefficients, RFR for real and random coefficients and RFA if the coefficients are real, random and non-zero for even n and zero for odd n).

4. Numerical analysis

With this knowledge, we can now proceed as follows. (i) Numerically compute the eigenfunctions by diagonalizing the matrix **U** (equation (2)); (ii) calculate their Bargmann transforms, using equation (8); (iii) numerically compute the position of each zero using Cauchy's integral (see [7]); (iv) use the so obtained N^2 zeros (N for each of the N eigenfunctions) to evaluate the various statistical measures. For the reasons explained above, we repeat steps (iii) and (iv) also for random functions cases, with normally distributed coefficients $\psi(q_n)$'s.

To see the effect of various parameters on the statistical behaviour of zeros, the above steps are repeated for many of their combinations. Here, until otherwise stated, we always take ($K = 20\,000$, $M = 1$, $N = 199$, $\gamma = 0.7071$, $\theta_0 = \pi/2N$) for the delocalized case with no symmetry, ($K = 20\,000$, $M = 1$, $N = 199$, $\gamma = 0.0$, $\theta_0 = \pi/2N$) for the delocalized case with one symmetry (time reversal), ($K = 20\,000$, $M = 1$, $N = 199$, $\gamma = 0.0$, $\theta_0 = 0.0$) for the delocalized case with two symmetries (namely time reversal and parity) and ($K = 10$, $M = 30$, $N = 199$, $\gamma = 0.7071$, $\theta_0 = \pi/2N$) for the localized case with no symmetry. To improve the statistics, we superimpose the statistics for N zeros of each of the N eigenfunctions and set $T = 1$.

We start by computing the density ρ of zeros, distributed over the phase plane of unit area. We know that the eigenfunctions of RM ensembles, in the Bargmann representation, have the form of the RPs. The nature of the coefficients in these polynomials depends on the symmetries of the ensembles (for example complex for no antiunitary symmetry and real for 1 antiunitary symmetry). Recently it was shown that the zeros for RP with complex coefficients are uniformly distributed in the phase space for any arbitrary N while, in the case with real coefficients, this uniformity no longer survives due to an increased concentration of zeros on the real axis [10]. The same should hold well for the eigenfunctions of quantum systems with strongly chaotic classical dynamics where a typical wavefunction randomly goes all over the phase space and has a uniform intensity distribution except for a few scars (high-intensity regions) [1, 2]. This expectation has its roots in the success of RMT in modelling 'quantum chaotic' spectra; we hope the same for 'quantum chaotic' eigenfunctions too. In fact, figure 1(a) which shows the distribution of 99×99 zeros of all 99 eigenfunctions of QKR ($K = 20\,000$, $M = 1$, $N = 99$, $\gamma = 0.7071$, $\theta_0 = \pi/2N$) strongly suggest the uniformity of density in the phase plane. The various parameters here are chosen so as to ensure the underlying classical dynamics to be strongly chaotic and removal of all symmetries from the quantum case [5, 11, 12]. Figure 1(b) shows the case with a chaotic classical dynamics while the quantum dynamics is localized in the momentum space ($K = 10$, $M = 30$, $N = 99$, $\gamma = 0.7071$, $\theta_0 = \pi/2N$). Here again the zeros seem to be randomly and uniformly distributed, except for an increased concentration on parity symmetry axis $q = 0.5$ (reasons explained later). The apparent randomness and uniformity of the distribution of zeros (away from the axis) in this case is indeed misleading and occurs due to the averaging effects produced by the superposition of many wavefunctions. In fact, figure 2(a), where the Husimi distribution of a single eigenfunction is plotted, shows that the zeros for the localized case, in general, form patterns; for few of the eigenfunctions, zeros seem to be localized too. It seems that the maximum intensity regions, in order to concentrate in some part of phase space, compel minimum intensity regions to distribute in an ordered way. This pattern formation of zeros is more obvious for the eigenfunctions of the localized dynamics with a symmetry (figures 2(b) and (c)). Figure 2(d) shows the Husimi plot of an eigenfunction for delocalized case. Here zeros of even a single eigenfunction seem to be uniformly distributed. In fact, the distribution approaches the uniformity in $N \to \infty$, i.e. the semiclassical limit (unlike the RMT case where uniformity exists for all N) and therefore mimics the behaviour of underlying strongly chaotic classical dynamics.

In order to see whether the density $\rho(p, q)$ is separable in variables p and q or not, we calculate the coefficient of correlation $C(m, n)$, defined as follows

$$C(m, n) = \frac{\langle p^m q^n \rangle - \langle p^m \rangle \langle q^n \rangle}{\sigma(p^m)\sigma(q^n)} \tag{10}$$

where $\sigma^2(r^m)$ is the variance of mth moment of the variable r. To see the effect of various parameters as well as the dimensionality, we calculate $C(m, n)$, $(m + n < 8)$, for the delocalized case with no symmetry, one symmetry and two symmetry respectively and also for the localized case with no symmetry, with each case studied for four values of N, namely, $N = 61$, 99, 149, 199. We find that, for all the parametric cases, the correlations between p and q variable decrease with N. In fact, the correlations for lower moments are much less than one sample error even for $N = 61$ (with $C(m, n) \leqslant 10^{-5}$ for $m + n \leqslant 5$ and sample error $= 10^{-2}$), thus indicating their near absence even for small N-values. The correlations for higher moments ($m + n > 5$) although not negligible for small N-values, they decrease rapidly with increasing N and can safely be assumed to be zero in the limit $N \to \infty$ (for example $C(4, 4) = 0.018 \pm 0.016$ for $N = 61$ and 0.003 ± 0.005 for $N = 199$,

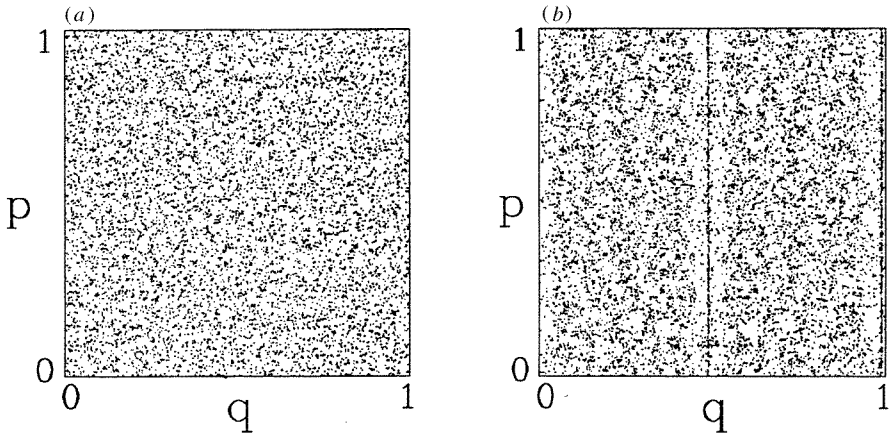

Figure 1. The superposition of the zeros of all eigenfunctions of U, (*a*) $K = 20\,000$, $M = 1$, $N = 99$, $\gamma = 0.7071$, $\theta_0 = \pi/2N$; (*b*) $K = 10$, $M = 30$, $N = 99$, $\gamma = 0.7071$, $\theta_0 = \pi/2N$.

for the delocalized case without symmetry). This implies that, for the delocalized as well as the localized case, we can study the distribution of zeros in either the p or q direction without taking care of the q or p variable, respectively. Thus, for a check on uniformity, it is sufficient to study the measure $\langle\rho\rangle_q$ and $\langle\rho\rangle_p$ (where $\langle\ \rangle_r$ implies the average over variable r). As shown in figures 3(*a*) and (*b*), the averaged density in both q (averaged over p) and p directions (averaged over q) for the delocalized case is nearly a constant, thus indicating a uniform distribution while, for the localized case, it oscillates strongly about an average value. Here the increased average density around some values of p and q implies the preference of zeros for this value; this behaviour may be attributed to the localization and pattern formation of zeros. For the delocalized case, the oscillation strength decreases rapidly with increasing N which indicates the uniform density also in the p direction, in the large-N limit. For comparison, we have also plotted the corresponding RF case in both figures 3(*a*) and (*b*); the set of normally distributed $\psi(q_n)$'s is generated by using 'GASDEV' subroutine [14]. Note the similarity of the delocalized case with the RF case in figures 3(*a*) and (*b*).

To see the effect of the symmetry on the distribution of zeros, we study it for various values of parameters γ and θ_0. Figures 4(*a*) and (*b*) show the distribution of the 61×61 zeros of all 61 eigenfunctions of QKR for ($K = 10$, $M = 30$, $N = 61$, $\gamma = 0.0$, $\theta_0 = 0$) and the case ($K = 10$, $M = 30$, $N = 61$, $\gamma = 0.0$, $\theta_0 = \pi/2N$). Here the first set of values correspond to the preservation of both T and P symmetries in the system whereas in the second case only T-symmetry is preserved. Figure 4(*a*) shows the increased density of zeros on the two symmetry axis (namely, $p = 0.5$ and $q = 0.5$) while in figure 4(*b*) the zeros are concentrated only on one symmetry axis; the concentration of zeros also on $p = 1.0$ is due to the torus boundary conditions. Moreover, zeros on either side of the symmetry axis seem to avoid it, thus creating a hole close to and around the symmetry axis. This phenomenon, which occurs in the case of RP (and RF) too, can be explained as follows. If $\psi(z_p) = 0$, then $\psi(Rz_p) = 0$, where R refers to a particular symmetry in the quantum system and Rz_p refers to the R-symmetry counterpart of z_p. This implies that, given z_p a zero of wavefunction ψ, Rz_p will also be its zero; zeros either come by pairs symmetric with respect to the symmetry axis or they are single and lie on the axis (see also a related work in [15]). Although this destroys the uniformity of distribution of

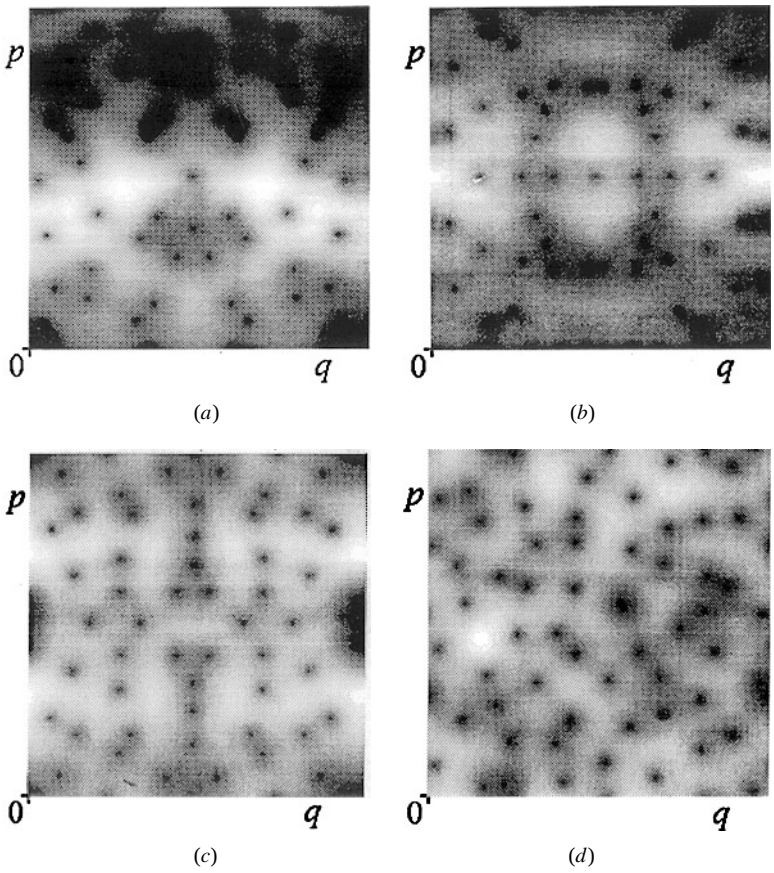

Figure 2. The Husimi distribution of a single eigenfunction, (*a*) $K = 10$, $M = 30$, $N = 61$, $\gamma = 0.7071$, $\theta_0 = \pi/2N$; (*b*) $K = 10$, $M = 30$, $N = 61$, $\gamma = 0.0$, $\theta_0 = 0.0$; (*c*) $K = 10$, $M = 30$, $N = 61$, $\gamma = 0.0$, $\theta_0 = 0.0$; (*d*) $K = 20\,000$, $M = 1$, $N = 61$, $\gamma = 0.7071$, $\theta_0 = \pi/2N$.

zeros on a global level, locally and away from the symmetry axis the uniformity is still preserved (figures 3(*c*), (*d*), 4(*a*), (*b*)). It should also be noted in figure 1(*b*) that although both γ and θ_0 are non-zero, the density of zeros is still higher along the $q = 0.5$ line while this behaviour is absent in the delocalized case for the same values of symmetry breaking parameters (figure 1(*a*)). It seems that for the localized case, a more generalized symmetry remains preserved even for non-zero values of γ and θ_0.

In order to analyse the correlations between these zeros as well as to know the extent of randomness, we compute the two-point correlation function $R_2(r)$. It is defined as the joint probability density of finding a zero at a radial distance x from the origin and another at $x + r$, averaged over all x and θ, where θ is the angular dependence of the zero. Here r is measured in units of averaged spacing and $R_2(r)$ is unfolded in such a way so that the average number of zeros at a distance r from a given zero does not depend on r. In [10], we analytically obtained $R_2(r)$ for zeros of RPs; a numerical comparison of this formulation with that for the kicked spin system as well as the kicked rotor showed an excellent agreement. Here we numerically compare $R_2(r)$ for delocalized QKR with that for the random functions (with complex coefficients to model the no-symmetry case

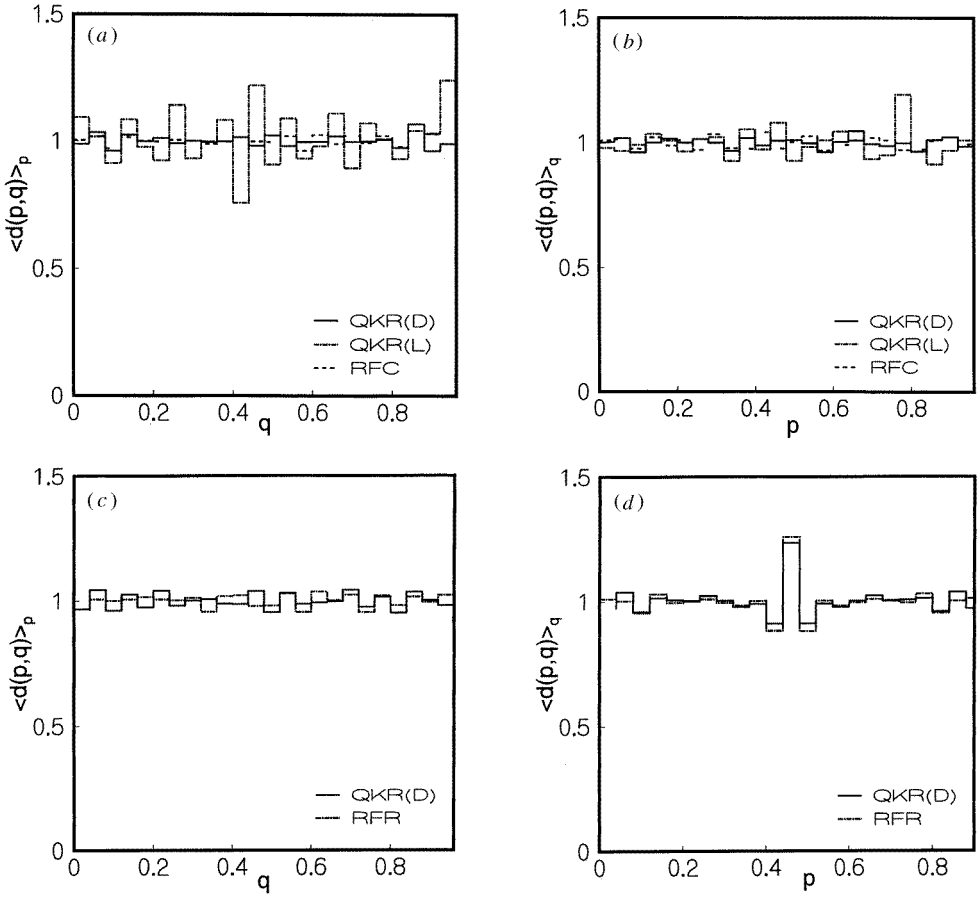

Figure 3. The density $\rho(q, p)$ of zeros in phase plane with respect to q (averaged over all values of p and measured in units of $\langle q \rangle$) and p (averaged over all values of q and measured in units of $\langle p \rangle$), (*a*) and (*b*) $K = 20\,000$, $M = 1$, $N = 99$, $\gamma = 0.7071$, $\theta_0 = \pi/2N$, (full curve), $K = 10$, $M = 30$, $N = 99$, $\gamma = 0.7071$, $\theta_0 = \pi/2N$, (broken curve), RFC case (dotted curve); (*c*) and (*d*) $K = 20\,000$, $M = 1$, $N = 99$, $\gamma = 0.0$, $\theta_0 = \pi/2N$, (full curve), RFR case (dotted curve).

and real coefficients for the time-reversal symmetry preserving case) and find the latter to be a good model for the former; see figures 5(*a*)–(*c*). The agreement of the results also confirms that zeros for both random polynomials and random functions, in $N \to \infty$, have similar correlations at least up to the second order. The histograms in figures 5(*a*)–(*d*) also indicate that, for short distances, the two-point correlation increases as a power law with distance, attains a maximum value and then oscillates rapidly around this average value when distances are large. Thus, for short distances ($r < 1$), zeros seem to repel each other; the repulsion is weaker for the localized case than the delocalized case (figure 5(*d*)). Furthermore, the presence of a symmetry weakens the repulsion at short distances but does not seem to affect the correlations at large distances (figures 5(*b*)–(*d*)) (but as shown later, long-range correlations are indeed symmetry dependent). Our comparison of short-range correlations under various symmetry conditions for many N-values (61, 99, 149, 199) seems to suggest the decreasing tendency of differences in the repulsion strength under

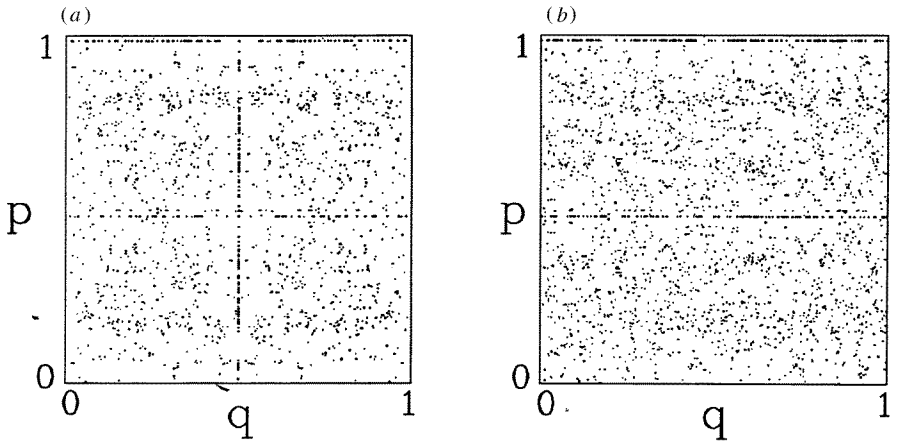

Figure 4. The superposition of the zeros of all eigenfunctions of U; (a) $K = 10$, $M = 30$, $N = 61$, $\gamma = 0.0$, $\theta_0 = 0.0$; (b) $K = 10$, $M = 30$, $N = 61$, $\gamma = 0.0$, $\theta_0 = \pi/2N$.

various parametric conditions with increasing N. We believe that no difference should survive in the $N \to \infty$ limit; this is also corroborated by our spacing study given later. Moreover, the short-range ($r < 1$) correlation between zeros is different from that for the two-dimensional random distribution of points with $R_2(r) = 1$ but behaves in a similar fashion for $r > 1$. Note here that the long-range behaviour for all the cases approaches 1, although oscillating heavily around it, irrespective of the parametric conditions or the type of the distribution. These oscillations are not insignificant; they should contain information about the differences in long-range correlations under various parametric conditions so as to agree with our number-variance study, given later.

The $R_2(r)$ study suggests that the short-range correlations are free from the influence of various parameters. To understand this better, we carry out a study for the nearest-neighbour spacing distribution $P(s)$ of zeros (with all geometrical factors scaled out; see [10]) for both QKR as well as RFs. A comparison of the two reconfirms the conclusion obtained by the $R_2(r)$ study, that is, the short-range fluctuation measures of zeros distribution of random functions can model very well that of QKR (figures 6(a)–(c)). To understand the functional behaviour of $P(s)$, we fit the following equation

$$P(s) = \alpha s^a \exp[-\beta s^b] \tag{11}$$

where a and b are the fitting parameters and α and β are obtained by imposing the following normalization conditions, $\int_0^2 P(s)\,\mathrm{d}s = 1$ and $\int_0^2 s\,P(s)\,\mathrm{d}s = 1$. The fitting analysis carried out for four values of $N = 61$, 99, 149, 199 leads us to expect $a = 1.5$ and $b = 5$. Using these values as a hypothesis for $P(s)$, we perform the χ^2-analysis which gives us $\chi^2 = 12.56$ for $N = 199$ and 14 degrees of freedom at a 5% level of significance, a value much less than the theoretical χ^2-value ($= 23.68$). This therefore indicates the correctness of our hypothesis. We also find that the calculated χ^2-value decreases with increasing N (e.g. $\chi^2 = 148.18$ for $N = 99$ and 14 degrees of freedom) which implies the tendency of $P(s)$ to approach our hypothesis in the $N \to \infty$ limit.

Our $P(s)$ analysis also shows that the short-range correlations between the zeros are not of the same type as those for a two-dimensional random distribution of points (with $P(s)$ being a two-dimensional Poisson distribution with $a = 0$ and $b = 2$ [10]). In fact, it has been indicated [8] that the appearance of a term of the type of general n-body interaction

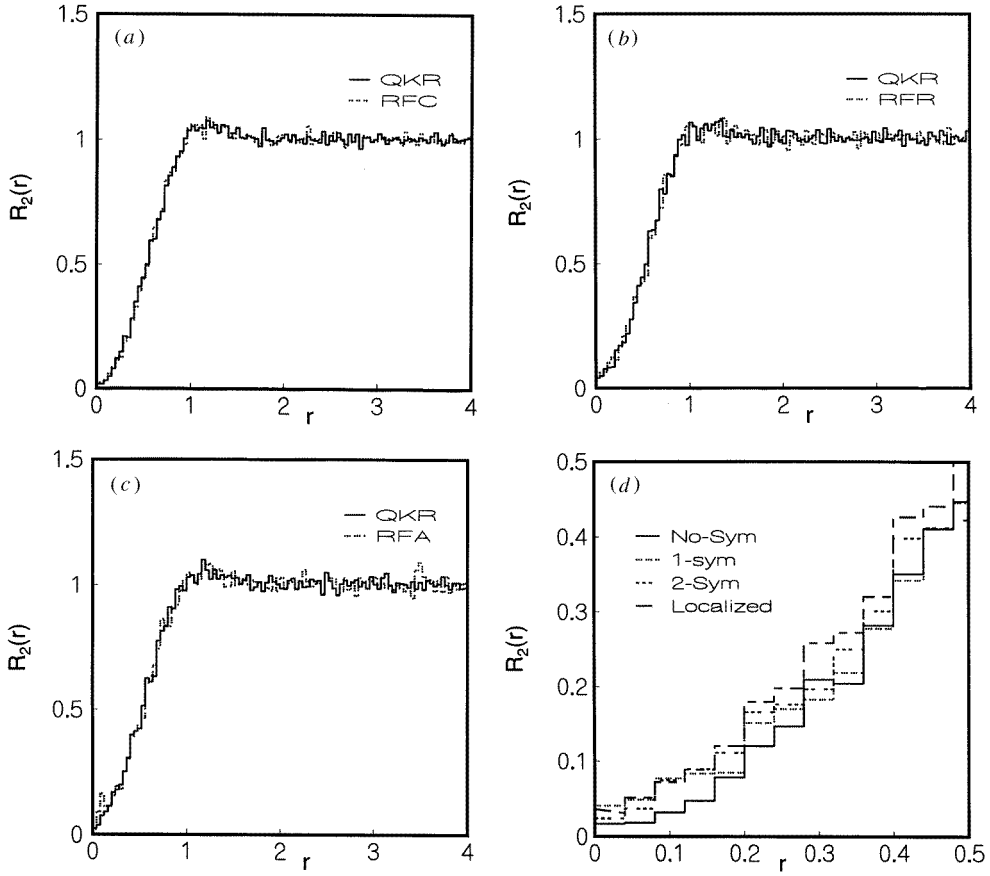

Figure 5. The histogram for two-point correlation function R_2 of the zeros (with unit mean spacing), (*a*) delocalized without any symmetry (full histogram) and RFC (dotted histogram); (*b*) delocalized with one symmetry (full histogram) and RFR (dotted histogram); (*c*) delocalized with two symmetries (full histogram) and RFA (dotted histogram); (*d*) with respect to small values of r, no-symmetry case (full line), one symmetry (dotted line), two-symmetry (small-broken line), localized case (large-broken line). Note here the difference between various curves is bigger than the finite-sample error ($\approx 5 \times 10^{-3}$) associated with each case.

in the dynamics of zeros should produce strong short-distance correlations among zeros. Furthermore, for finite N-cases, the repulsion between these zeros for small distances is stronger for the localized case than the delocalized case. The presence of the repulsion leads zeros of the delocalized case to distribute uniformly in the phase space but the distribution is not a random one. In the localized case too, the existence of a stronger repulsion may be the cause of the pattern formation of zeros. Again the presence of a symmetry affects the spacing distribution for small-s values, by increasing the probability of small-spacings relative to the no-symmetry case (figure 6(*d*)); this happens due to many very close-lying zeros on the symmetry axis. But our analysis for various N-values indicates the tendency of this probability to decrease with higher N, approaching the same behaviour as in the no-symmetry case (i.e. equation (14)) in the $N \to \infty$ limit. This is what we expect as the fraction of zeros ($N^{+1/2}$) on the symmetry axis vanishes in the semiclassical regime. The fitting analysis followed by the χ^2-analysis further confirms that, in the $N \to \infty$ limit,

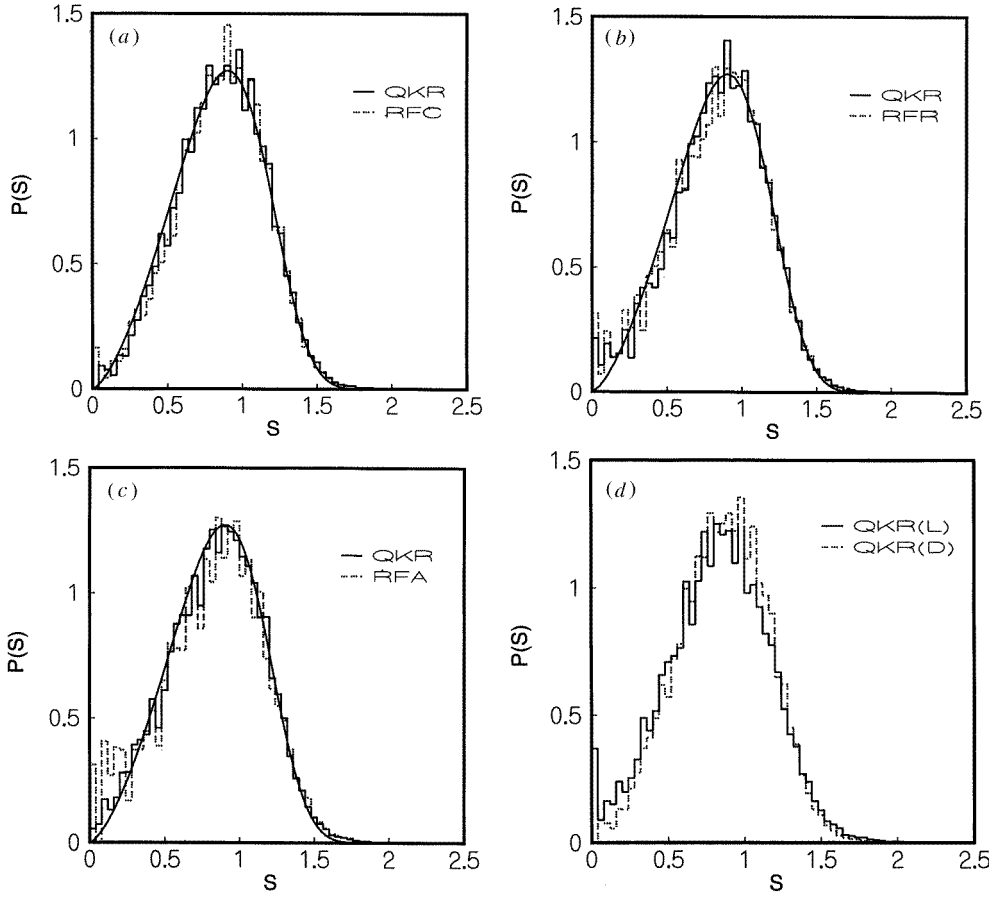

Figure 6. The histogram for nearest-neighbour spacing distribution (with unit mean spacing) (*a*) delocalized without any symmetry (full histogram) and RFC (dotted histogram); (*b*) delocalized with one symmetry (full histogram) and RFR (dotted histogram); (*c*) delocalized with two symmetries (full histogram) and RFA (dotted histogram); (*d*) localized case with no symmetry (full histogram) and delocalized case with no symmetry (dotted histogram). Here the full curve in (*a*)–(*c*) is the fitting given by equation (14).

$P(s)$ is not affected by the presence or absence of a symmetry, localization or delocalization of quantum dynamics and can be described by equation (11). The calculated χ^2-value, if equation (11) is taken as a hypothesis, is 12.56, 18.24 and 30.78 for 14 degrees of freedom of one symmetry, two symmetry and the localized cases respectively. This is much less than the theoretical $\chi^2 (= 23.68)$ at the 5% level of significance for the first two cases, thus indicating correctness of our hypothesis. For the last case, although the observed value is much greater than the theoretical one even for $N = 199$ but again the decreasing χ^2 with increasing N (for example $\chi^2 = 199.65$ for $N = 99$ and 14 degrees of freedom) suggests the validity of equation (11) in the $N \to \infty$ limit for this case too.

The $R_2(r)$ study does not inform us much about the effect of various parameters on long-range correlations. We study, therefore, another fluctuation measure, namely, the 'number variance' $n(r)$ which is defined as the variation in the number of zeros in an area of size r^2, where r^2 is sufficiently large to include many zeros on an average and its two-

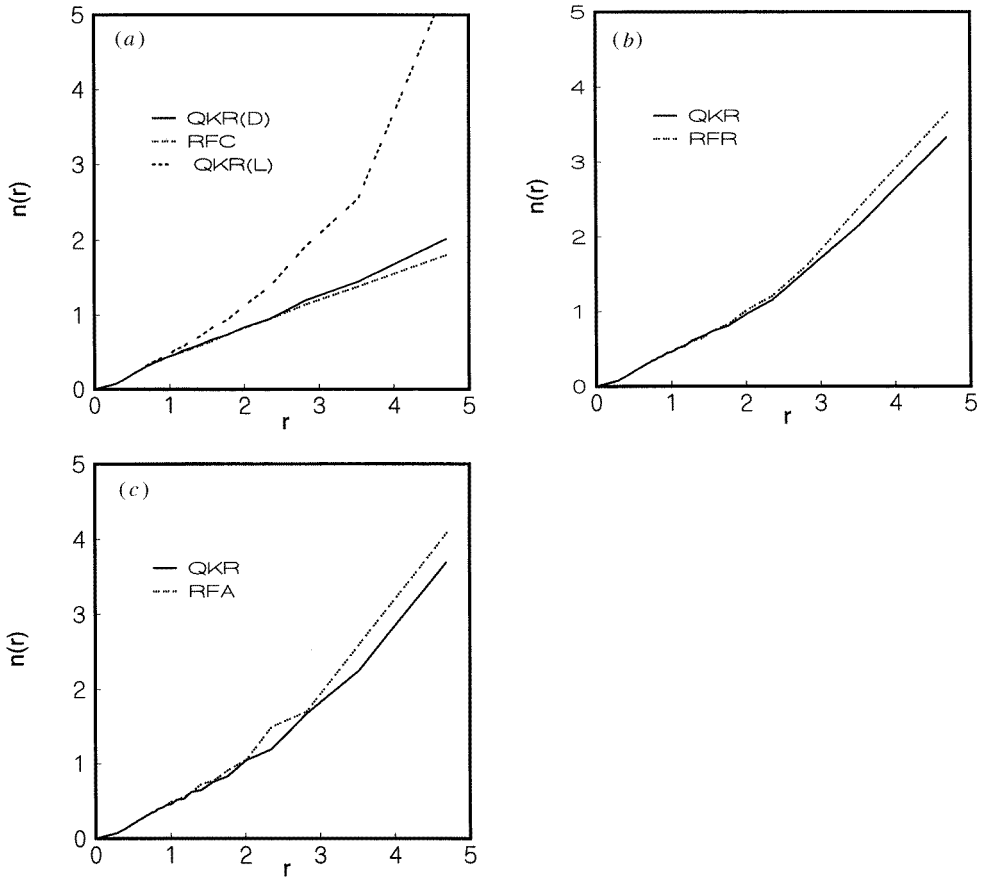

Figure 7. Number variance $n(r)$, (*a*) delocalized without any symmetry (full curve), localized case (broken curve) and RFC (dotted curve); (*b*) delocalized with one symmetry (full curve) and RFR (dotted curve); (*c*) delocalized with two symmetries (full curve) and RFA (dotted curve).

dimensional analogue of the number variance quite often used for spectrum studies. For a random distribution of points distributed on a unit plane (with no correlation among them), the variance increases as r^2. if the variance remains smaller than r^2 as the mean number of zeros increases, the existence of a long-range correlation in the spectrum is indicated. Figure 7 shows that the variance in the number of zeros for large r is increasing with r; the rate of increase, for both QKR and RF, is much slower than that of the random distribution of points. This reflects that long-range correlations are indeed present among zeros of both QKR and RF, although stronger in the former as compared with the latter, if the dynamics is localized or symmetries are present (figures 7(*a*)–(*c*)); the reverse is true if the dynamics is delocalized with no symmetry (figure 7(*a*)). As can be seen from figure 7, these correlations are strongest for delocalized dynamics with no symmetry, a little weaker for symmetry cases and weakest for localized cases. A similar tendency was also seen in the case of the eigenvalues [5, 12]; the presence of a symmetry or localization of dynamics results in weakening of the long-range correlations with a tendency to behave as in the case of Poisson distribution. (This should not be surprising as the Poisson distribution results are due to a large number of symmetries present in the system.)

In this paper, we have attempted to gain an insight into the complex world of wavefunctions by numerically analysing the distribution of their zeros. Although the studies here have been carried out for only one system, we believe in the general applicability of results obtained here. Our study indicates that the zeros for strongly chaotic cases tend to acquire a uniform distribution in the phase space in the limit $N \to \infty$; this distribution is different from that of the set of random points. The analysis of various fluctuation measures shows that, in the large N-limit, the short-range correlations of zeros of quantum chaotic systems are universal, parametric independent and have the same nature as those for the random functions case or random polynomials but long-range correlations seem to differ. We expect the nature of this deviation to be system dependent; this expectation has its roots in the earlier observation of a similar tendency in the eigenvalues case. Again, the localization versus delocalization phenomena of quantum state reveals itself in the statistical behaviour of zeros too. The presence of a symmetry induces the changes in the distribution of zeros and also modifies the long-range correlations. This again confirms that zeros contain a lot of information about the underlying classical as well as quantum dynamics and therefore can be used to gain a better understanding of the subject. But we have not as yet extracted all the information about zeros. For example, we still have to understand how the motion of zeros is affected by the variation of various parameters of the system. We also need to analyse higher-order correlations which can tell us more about their parametric and system dependence. It is also desirable to have a complete analytical formulation of statistical properties of these zeros as it will help us gain a better understanding of wavefunctions.

Acknowledgments

I am grateful to A Voros for suggesting the problem and for the numerical programme to compute the zeros in phase space. I also wish to express my gratitude to P Leboeuf, and O Bohigas for many fruitful discussions and Jawaharlal Nehru Centre for advanced research (JNCASR) for their computing facility and economic support.

References

[1] Berry M V 1977 *J. Phys. A: Math. Gen.* **10** 2083
[2] Heller E J 1984 *Phys. Rev. Lett.* **53** 1515
also Heller E J 1986 *Quantum Chaos and Statistical Nuclear Physics (Mexico) (Lecture Notes in Physics 263)* ed T H Seligman and H Hishioka (Berlin: Springer)
[3] Bogomolny E B 1988 *Physica* **31D** 169
[4] Casati G and Molinari L 1989 *Prog. Theor. Phys. Suppl.* **98** 287
[5] Shukla P 1992 *PhD Thesis* Jawahar Lal Nehru University, New Delhi
[6] Haake F 1991 *Quantum Signature of Chaos* (Berlin: Springer)
[7] Leboeuf P and Voros A 1990 *J. Phys. A: Math. Gen.* **23** 1765
Leboeuf P and Voros A *Quantum Chaos* ed G Casati and B Chirikov (Cambridge: Cambridge University Press)
[8] Leboeuf P 1991 *J. Phys. A: Math. Gen.* **24** 4575
[9] Bogomolny E, Bohigas O and Leboeuf P 1992 *Phys. Rev. Lett.* **68** 2726
[10] Leboeuf P and Shukla P 1996 *J. Phys. A: Math. Gen.* **29** 4827
[11] Izrailev F M 1986 *Phys. Rev. Lett.* **56** 541
[12] Pandey A, Ramaswamy R and Shukla P 1993 *Ind. J. Phys.* **41** L75
Shukla P and Pandey A 1997 *Nonlinearity* to appear
[13] Voros A 1989 *Phys. Rev.* A **40** 6814
[14] Press W H *et al Numerical Recipes* (Cambridge: Cambridge University Press)
[15] Braun D, Kuś M and Życzkowski K 1997 *J. Phys. A: Math. Gen.* **30** L117